Received: 15 July 2024 | Revised: 14 November 2024 | Accepted: 24 December 2024

DOI: 10.1002/met.70027

Meteorological Applications
Science and Technology for Weather and Climate
Open Access
RMetS

RESEARCH ARTICLE

Unveiling meteorological synergies in the coupling of an abnormal easterly wave and cutoff low in South Africa's February 2023 rainfall

Farahnaz Fazel-Rastgar[1] | **Venkataraman Sivakumar**[2] | **Masoud Rostami**[3,4] | **Bijan Fallah**[5]

[1]School of Chemistry and Physics, University of KwaZulu Natal, Durban, South Africa

[2]S.V. Raman Researchers Roadmap, Durban, South Africa

[3]Potsdam Institute for Climate Impact Research (PIK), Member of the Leibniz Association, Potsdam, Germany

[4]Laboratoire de Météorologie Dynamique (LMD), Sorbonne Université (SU), Ecole Normale Supérieure (ENS), Paris, France

[5]Deutsches Klimarechenzentrum GmbH (DKRZ), Hamburg, Germany

Correspondence
Masoud Rostami, Potsdam Institute for Climate Impact Research (PIK), Member of the Leibniz Association, P.O. Box 60 12 03, D-14412 Potsdam, Germany.
Email: rostami@pik-potsdam.de, masoud.rostami@lmd.ipsl.fr

Funding information
Virgin Unite USA, Inc. through the Planetary Boundary Science Lab project

Abstract

This study seeks to understand the meteorological mechanisms that caused widespread and heavy rainfall from 6 to 14 February 2023, over southern Mozambique and the eastern and northeastern areas in South Africa, including Limpopo Province, Mpumalanga Province and northern KwaZulu-Natal, by examining different outputs from reanalysis datasets. The heavy rainfall had a substantial hydrological impact, leading to significant flooding and disruptions. This research revealed that a slow-moving cutoff low (COL) system remained over the central parts of South Africa, triggering extensive and heavy rainfall mostly over the northeastern and eastern provinces. The outcomes from the reanalysis datasets display the influence of the weather system and the interaction between an initiated westerly wave, which converted into a near-stationary upper-air cold core upper air COL system, and the easterly wind wave associated with the South Indian Ocean Convergence Zone (SICZ), bringing significant warm humid air from the Indian Ocean into the study area. This study revealed an abnormal structural pattern in the wind vectors, low-pressure trough, upper and mid-tropospheric westerly flows and humidity compared with the long-term climate normal values over Mozambique and the northeastern and eastern regions of southern Africa. This event is exciting from a meteorological perspective due to its intensity and duration, the involvement of cyclonic activity and its implications for understanding the impacts of climate change on weather patterns in southern Africa. The heavy rainfall had a substantial hydrological impact, leading to significant flooding and disruptions, providing valuable data for improving forecasting models and disaster preparedness strategies and underscoring the importance of enhancing climate resilience in regions prone to extreme weather.

KEYWORDS

COL, easterly waves, heavy rainfall, Mozambique Channel Trough, southeastern Africa

1 | INTRODUCTION

The Mozambique Channel Trough (MCT) is notable for its cyclonic activity, which becomes particularly prominent in the central and southern regions during the austral summer (Barimalala et al., 2018). The Mozambique Channel is a channel in southeastern Africa between Mozambique and Madagascar. The trough generally forms in December and reaches its highest intensity in February. During this period (December to February), the Mozambique Channel is typically warmest, and the Mascarene high pressure is placed farthest southeast of the Indian Ocean basin (Barimalala et al., 2020). The Madagascar topography and the intensity of the MCT regulate the summer rainfall in southern Africa (Barimalala et al., 2018, 2020). During the strong MCT, the moisture bringing easterlies from the South Indian Ocean delayed the penetration of Mozambique, causing less precipitation. However, during the weakness of the MCT, rainfall may increase in South Africa during summer. The Southwest of the Indian Ocean is one of the key factors for South African precipitation because it is the main moisture source for the region (Cook, 2000; Hoell et al., 2017; Landman & Mason, 1999; Ordóñez et al., 2012; Reason & Mulenga, 1999). Additionally, moisture can be transferred onshore with trade winds from the Mascarene high-pressure system (Rapolaki et al., 2021; Xulu, 2017). An important aspect is atmospheric blocking through the Mascarene High, which leads to anomalous temperature and precipitation over the subcontinent. This blocking results in the landfall of tropical cyclones and the slow transmission of the cutoff low (COL). This causes severe weather and subcontinent flooding (Xulu et al., 2020). The formation of the COLs in this area is distinctive in terms of both their severity and occurrence during the year (Singleton & Reason, 2007a, 2007b; Weldon & Reason, 2014).

Severe rainfall and its variability in southern Africa are strongly affected by the formation of midlatitude weather features such as a COL system (Barnes et al., 2021; Fazel-Rastgar & Sivakumar, 2022; Reason, 2017; Singleton & Reason, 2007a, 2007b; Sivakumar & Fazel-Rastgar, 2021; Xulu et al., 2023). However, the Madagascar topography, the MCT intensity (Barimalala et al., 2020) and the easterly waves associated with internal tropical convergence zones can also alter the summer rainfall over southern Africa (Cook, 2000; Dieppois et al., 2016; Nicholson, 2003; Seo et al., 2008; Xulu et al., 2020). Additionally, limited work has been conducted on the effect of the MCT on the mean state of precipitation in the southern African region, especially with high spatial and temporal resolution rather than large-scale climatology.

During summer, strong MCT activity is illustrated by considerable cyclonic circulation over the Mozambique Channel, emerging to the midlatitudes of South African regions. These findings are promising for tropical–extratropical cloud band development over the southwestern Indian Ocean. This initiates a rainfall increase over the ocean but a decrease in the southern African mainland. However, a weak MCT occurs with strong positive southern Indian Ocean subtropical dipole motion, which results in more rainfall being received in the subcontinent. At the same time, Madagascar and northern Mozambique are anomalously dry with less precipitation (Barimalala et al., 2020).

An easterly wave is defined as an inverted trough with an elongated area of a relatively low-pressure air system in the lower troposphere, causing cloudiness and developing thunderstorm clusters such as mesoscale convective systems (Rostami & Zeitlin, 2021). An easterly wave is a perturbation that spreads into the west with a speed of approximately 5–10 m/s (following low- and mid-level easterly flows) over the east wind trade. It slopes with a reversed 'V' shape to indicate a trough associated with the cyclonic vorticity, mostly over the atmospheric levels of 700 and 850 hPa. The easterly wave curvatures connect with an increase in convection, which results in rainfall. The saturation of the instability in the 'dry' case is due to subharmonic interactions. It is, therefore, sensitive to boundary conditions, with the most unstable mode of the jet exhibiting a meridional asymmetry (Rostami & Zeitlin, 2021). Organized convection boosts cyclonic vorticity in the system, initiating the cyclogenesis process. The African easterly waves (AEW) is a subcategory of easterly waves originating in Africa (Burpee, 1972; Riehl, 1944). These waves obtain cyclonic vorticity from the mid-level African easterly jet between the North Sahel and southern Saharan Desert. Recent studies have further explored the impacts of climate change on extreme weather events and patterns in various regions, including Central Asia, providing valuable insights into how such changes could influence weather systems similar to the MCT (Fallah et al., 2023, 2024; Fallah & Rostami, 2024). The changes in the trade winds are insignificant in the belt of the trade winds. However, they can be accompanied by heavy rainfall, specifically over the west sides of the oceans, such as the Atlantic Ocean and the Caribbean. Rainfall is commonly controlled by a wavelike participation of the normal isobaric pressure pattern called easterly waves (Burpee, 1972; Chang, 1972; Riehl, 1944). For example, the AEW can originate from strong convection in tropical North Africa, Ethiopia, Kenya and South Sudan. These waves obtain cyclonic vorticity for rotation from the mid-level African easterly jet between the North Sahel and southern

Saharan Desert. Additionally, the strongest deep cloud activity associated with deep convection is located in the area with the highest sea surface temperature, suggesting a correlation between sea surface temperatures, the Intertropical Convergence Zone and the surface wind confluence (Tai & Ogura, 1987).

Earlier studies over eastern Africa and the western coast of India rainfall pattern have shown a positive correlation during the summer (Hulme, 1992).

It is noted that the tropical and subtropical convergence zones, such as the South Pacific, South Atlantic and South Indian Ocean Convergence Zones (SICZs), are influential descriptions of the Southern Hemisphere climate during austral summer (Barimalala et al., 2018; Carvalho et al., 2004; Cook, 2000; Kiladis et al., 1989). In the southern African region, the SICZ plays a key role in the Austral summer precipitation (Cook, 2000). The Madagascar topography through the MCT has an important role in the direct moisture transport from the Indian Ocean toward southern Africa that may enhance SICZ (Barimalala et al., 2018).

The southwestern Indian Ocean is a critical factor for South African precipitation as it is the primary moisture source for the region (Cook, 2000; Hoell et al., 2017; Landman & Mason, 1999; Ordóñez et al., 2012; Reason & Mulenga, 1999). Additionally, trade winds from the Mascarene high-pressure system can transport moisture onshore (Rapolaki et al., 2021; Xulu, 2017). Atmospheric blocking by the Mascarene High leads to anomalous temperature and precipitation over the subcontinent. This blocking results in the landfall of tropical cyclones and the slow progression of the COL, causing severe weather and flooding (Xulu et al., 2020). The formation of COLs in this area is notable for both their severity and frequency (Singleton & Reason, 2007a, 2007b; Weldon & Reason, 2014).

This study aims to investigate the interaction between easterly waves associated with the SICZ and a COL system across the study area. Also, the objectives of this research by characterization of this case study, such as the volume of rainfall, duration and regions affected, can be considered as the main economic and social consequences. It may impact a better potential forecast when such floods may occur again.

2 | METHODOLOGY AND DATA

This study uses climate reanalysis model datasets from the National Centers for Environmental Prediction and the National Center for Atmospheric Research (NCEP–NCAR). The reanalysis model (Kalnay et al., 1996) conducts global gridded weather and climate data. Data assimilations are conducted using the model and observation, incorporating various meteorological and physical parameters. Those data from radiosondes, surface observations, dropsondes, radiosonde balloons, pilot balloons, polar orbit and geostationary satellites are available from 1948 to the present.

Composite mean maps and anomaly charts were developed with software support from the National Oceanic and Atmospheric Administration/Earth System Research Laboratories NOAA/ESRL Physical Sciences Division (www.esrl.noaa.gov/psd). The spatial coverage of the NCEP reanalysis is 2.5° × 2.5° and the global (Lat/Lon) grids of 144 × 73 cover from 0.0°E to 357.5°E and 90.0°N to 90.0°S. Daily mean composite values such as geopotential height, mean sea level pressure (SLP), isotherms, relative humidity, omega, zonal and meridional winds and wind vectors were calculated as the average variable over the study period (6–14 February 2023). Anomalies were defined as the daily average deviations from the climate normal values (1991–2020), which are used as a standard reference for evaluating long-term climate change.

Additionally, time- and area-averaged data for the study period were obtained from NASA's Modern-Era Retrospective Analysis for Research and Applications (MERRA) model (Rienecker et al., 2011). This study also utilizes ERA5 hourly data (Hersbach et al., 2020) from the European Centre for Medium-Range Weather Forecasts (ECMWF).

All calculations were based on the NCEP–NCAR Reanalysis model and other datasets. Daily composite maps are the averages of the mean (considered every 6 h a day) for each grid point in the model, and the anomalies are evaluated (mean − total base mean). The long-term climatology means are based on values from 1991 to 2020 as a reference base.

3 | STUDY AREA

Figure 1a depicts a map of the study area, encompassing South Africa and its bordering countries, along with the Mozambique Channel, situated between Mozambique and Madagascar in southeastern Africa. This region is significant due to the presence of the Mozambique Current, a warm surface current originating from the western Indian Ocean (Britannica & Editors of Encyclopaedia, 2023, https://www.britannica.com/place/Mozambique-Current). The southeast trade winds, influenced by the Earth's rotation, divert towards the Indian South Equatorial Current and then flow along the eastern coast of Africa. Part of this airflow passes through eastern Madagascar, while the remainder traverses

(a) (b)

FIGURE 1 Geographic map of South Africa showing the location of the Mozambique Channel (a) and South Africa map with provinces (b).

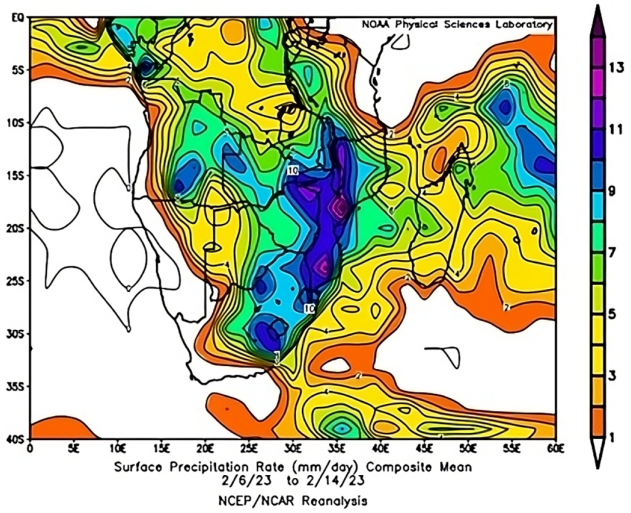

FIGURE 2 Precipitation rate (in millimetres per day) resulting from the NCEP reanalysis model during 6–14 February 2023 over the study area. NCEP, National Centers for Environmental Prediction.

westward through the Mozambique Channel. The Mozambique Channel exerts a profound not only climatological influence but also the economical inspiration as an important route for shipping in eastern Africa. Figure 1b shows the South Africa map with provinces.

4 | RESULTS

4.1 | Precipitation observed during 6–14 February 2023 over South Africa

Eastern and northeastern areas of South Africa have experienced heavy rainfall from 6th to 14th February 2023. This intense precipitation caused widespread flooding in several locations, including Kruger National Park, Lowveld, southern Kruger National Park, Crocodile Bridge and the main road connecting Skukuza to Lower Sabie. Figure 2 displays the precipitation rate (mm/day) derived from the NCEP reanalysis model during 6–14 February 2023 over the study area. The figure illustrates high precipitation rates predominantly over the northeast and eastern coastal areas and in the eastern parts of North–West and Eastern Cape provinces, with a maximum of 10 mm/day. Observed rainfall accumulations (mm) over South Africa from 6 to 12 February 2023 which was reported (Medrel 13 February 2023) by the South African Weather Service (SAWS) indicate severe precipitation, particularly affecting the eastern and northeastern provinces, including Gauteng, Limpopo, Free State, Eastern Cape and KwaZulu-Natal. For instance, Charters Creek in KwaZulu-Natal Province reported 242 mm from 11 to 12 February (morning), while Tshivhasie Tea Estate in Venda, Limpopo Province, recorded 294 mm from 10 to 11 February 2023.

Figure 3 depicts EUMETSAT images covering South Africa on 6 February 2023 at 0000Z (a) and 7 February 2023 at 0000Z (b), illustrating the weather system's evolution before and after the onset of continuous heavy precipitation. The precipitation rate is indicated in the figure legend. In Figure 3a, the impact of the SICZ and active westerly waves on the northern borders of South Africa is evident. The SICZ is a large-scale precipitation band feature over southern Africa accountable for the common austral summer precipitation that occurs from December to February (Cook, 2000; Todd & Washington, 1999).

4.2 | Synoptic weather observation

Figure 4 shows daily geopotential height maps at a level of 500 hPa during 6–14 February 2023 (Figure 4a–i) over

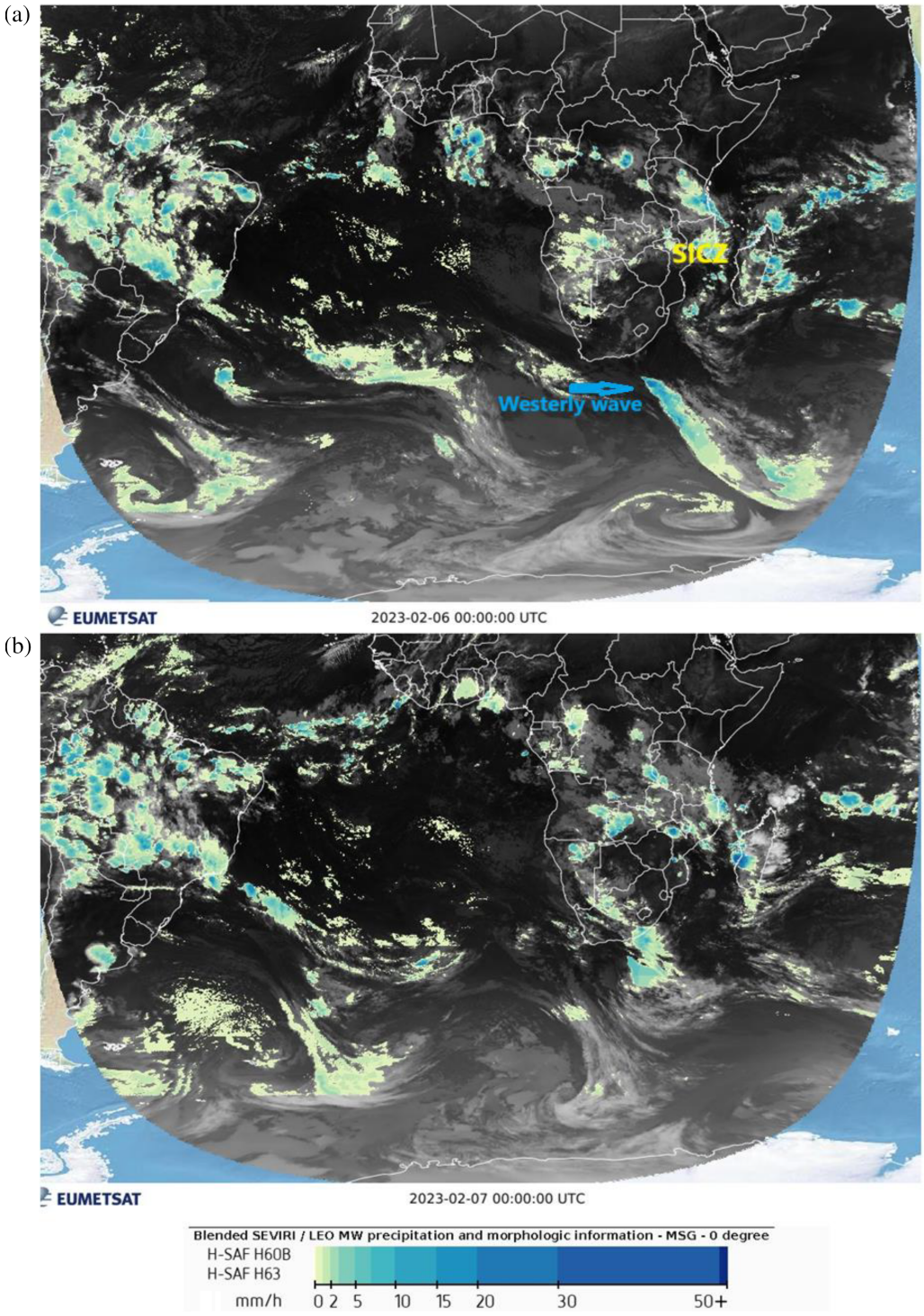

FIGURE 3 EUMETSAT image on6 February at 0000Z (a) and the image on 7 February 2023 at 0000Z (b) over the study area.

the study area. Figure 4a shows the development of an intense westerly wave originating from south-high latitudes toward the southwestern and western boundaries of South Africa on 6 February 2023. During this time, a closed mid-tropospheric low cell (centred at 584 pm) associated with the MCT was observed between Madagascar and Mozambique over the Mozambique Channel region (Figure 4a). A prominent cyclonic circulation zone is linked to the development of easterly wave perturbations during the austral summer over Mozambique (see next section). This closed low cell was surrounded by two upper anticyclonic centres (Namibia and the western Indian Ocean) observed by 6th February 2023. By the following day, the southern westerly wave

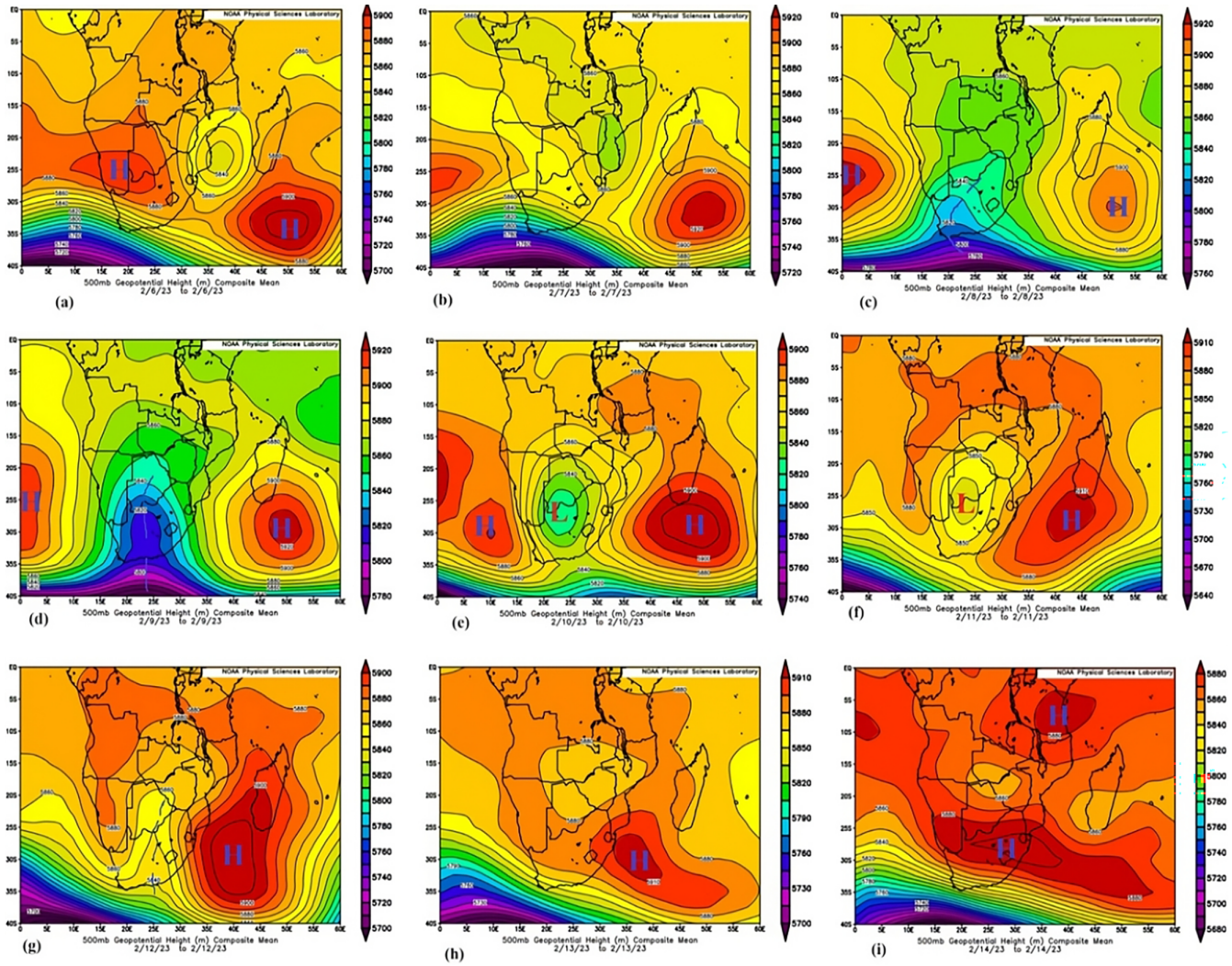

FIGURE 4 Daily geopotential height maps at 500 hPa during 6–14 February 2023 (a–i) respectively over the study area.

moved further toward the western part of South Africa on 7 February 2023 (Figure 4b). The westerly trough was located over the western boundaries of South Africa. On 8 February, the westerly trough curved in two different directions: the lower side shaped southwesterly (back) and the upper side tilted easterly, indicating the possibility of backward winds (Figure 4c). As expected, the following day (9 February 2023), a deep and straight southeasterly trough developed and impacted South Africa (see the dashed blue line in Figure 4d). This pattern triggered the formation of the upper air COL system over the study area by separating the upper side of the wave from the base part (Figure 4d–f). This pattern was associated with the development of intense severe weather systems, mainly over the eastern part of South Africa (see Figure 5). Due to the slow-moving characteristics of the COL, persistent rainfall over several days likely caused widespread flooding over the eastern, central and southeastern areas of South Africa (see Figure 2). On 12 February 2023, the COL converted to an open westerly trough, which was expected to move quickly (with a straight axis) toward the east (Figure 4g). Figure 4h shows the decay of the mentioned COL and the establishment of the normal seasonal anticyclonic high system over most of the study area, except for some small areas in the southwest affected by a new westerly wave (Figure 4h,i). However, from 13 to 14 February 2023, the 500-hPa geopotential height pattern shows a typical Mozambique cyclonic region, which is prominent during summer in the central and southern Mozambique Channel.

Figure 5a–i show the mean SLP during 6–14 February 2023. Figure 5a indicates the development of a low-pressure system with two closed cells of 1010 mb. The first cell, in the form of a nondynamic low (accompanied by an upper high), is located over the western part of South Africa. The second cell is elongated from the Mozambique Channel to the northeast of the study area

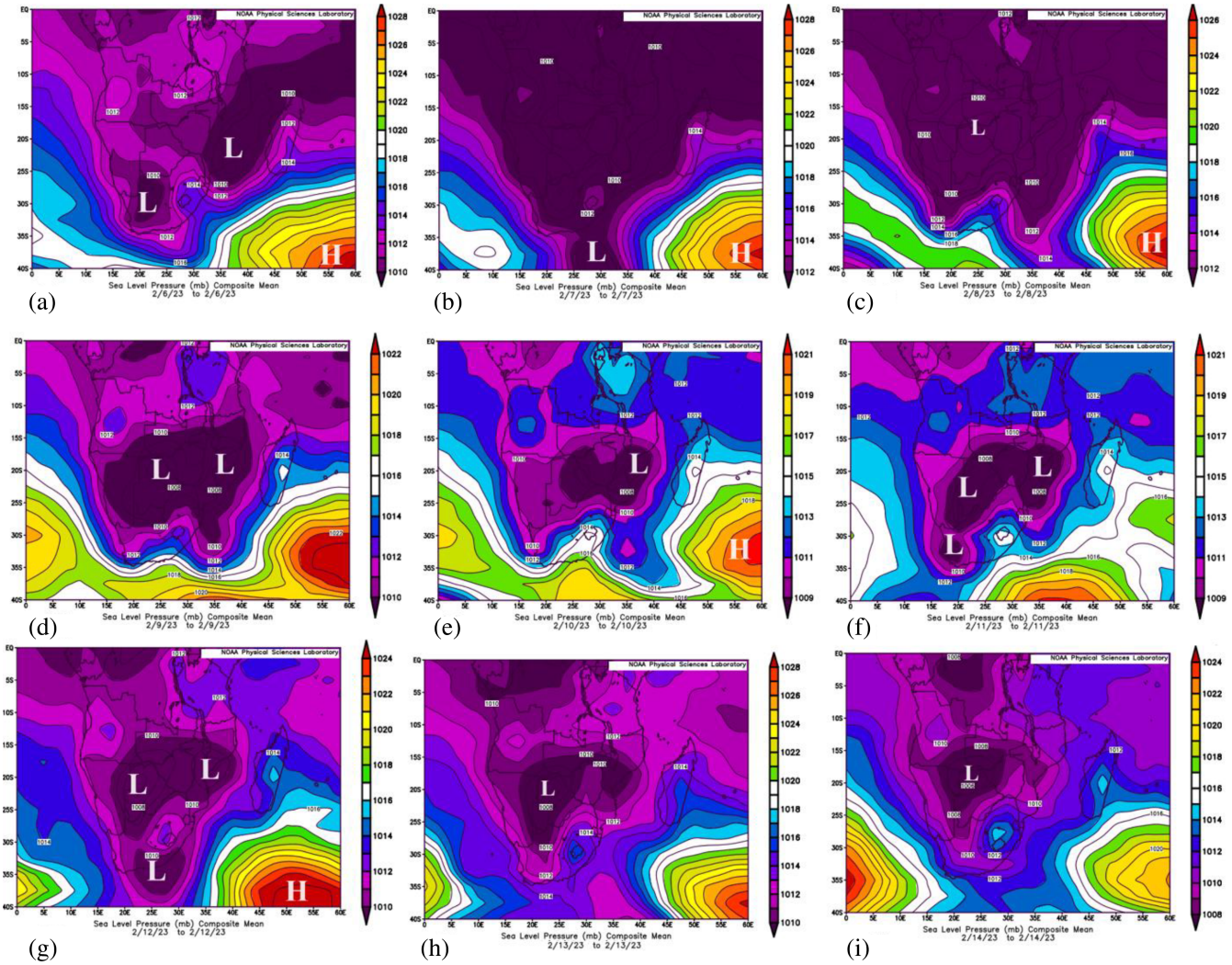

FIGURE 5 Composite mean map of the mean SLP during days 6–14 on February 2023. SLP, sea level pressure.

and is accompanied by an upper closed low (see Figure 4a), forming a dynamic low-pressure system. Between these two low-pressure systems, the anticyclonic high pressure (Indian Ocean Subtropical High) has curved to the northeast and east of the study area, causing a significant pressure gradient over these areas.

The Indian Ocean Subtropical High (IOSH), also known as the Mascarene High (MH), is located between 20°S–40°S and 45°E–100°E near the Mascarene Islands in the southern part of the Indian Ocean. Consequently, the eastern and northeastern areas of the study region are impacted by an active dynamic system causing disturbances over southern Mozambique and the northeastern and eastern areas.

Over the next 2 days, due to the intensification of the upper low and the deepening of its slow-moving trough (see Figure 4b,c), the instability over the study area persisted. On 9 February 2023, the low-pressure system intensified (centred at 1008 mb), accompanied by the formation of the upper COL on 10 and 11 February 2023. On 12 February 2023, the pressure slightly increased (by 2 mb) across the study area (Figure 5g). During the next 2 days (13 and 14 February 2023), the penetration of the Indian high-pressure tongue toward the eastern areas led to a decrease in low pressure. This was also accompanied by the weakening of the upper low and its replacement by the upper anticyclonic high over the study region.

A comparison with an average map of the 500-hPa composite mean during 6–14 February 2023 and average climate values as an anomaly map (Figure 6a) shows a stronger subtropical ridge centred (with a maximum of 60 gpm) over the southern Indian Ocean extending toward the Mozambique Channel. This occurs along with a deeper cyclonic low system (40 gpm) at the mid-tropospheric level centred over southern Botswana and northwestern South Africa (Figure 6a). This is accompanied by more intense low-level pressure (see the mean

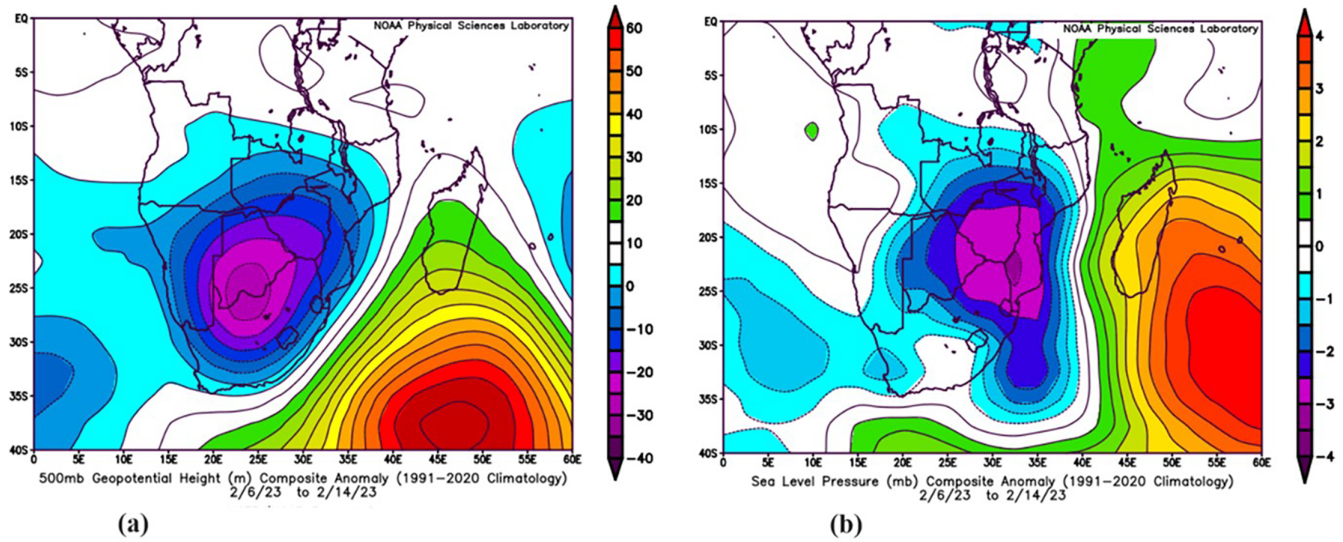

FIGURE 6 Anomaly map of the 500-hPa composite mean (a) and mean SLP anomalies (b) during 6–14 February 2023 over the study region. Anomalies are a departure from climate normal (1991–2020). SLP, sea level pressure.

SLP anomalies in Figure 6b) with a maximum of less than 4 mb over southern Mozambique and a stronger (with a maximum of 4 mb) Indian Ocean high-pressure system. This is accompanied by more substantial high pressure in Madagascar extending toward Mozambique and northeast South Africa. Therefore, the stronger ridge has been displaced and extended eastward to the study area, which favours easterly waves entering the study area and interacting with the westerly wave that fuels the SICZ (see the next section).

As a result, the stronger ridge has been displaced and extended eastward to the study area. This shift is significant as it favours the entry of easterly waves into the study area and their interaction with the westerly wave that fuels the SICZ (see the next section). This interaction could potentially have a profound impact on the weather patterns in the study area, which is a key finding of our research.

4.3 | Horizontal distribution of potential vorticity and ozone mixing ratio

One of the key indicators illustrating the development of meteorological conditions is the series of potential vorticity (PV) patterns at the 300-hPa isobaric level from 6 to 14 February 2023 (daily figures not presented here). On the first day of the study period, there was no significant PV observed over the study area. By 7 February, a slight southward penetration of the PV contours was noticeable over the eastern region, centred at Lesotho (∼−1.1 PVU). The potential vorticity unit (PVU) is equivalent to 10^{-6} km^2 kg^{-1} s^{-1}.

Data from the ECMWF ERA5 hourly data indicated high absolute PV values exceeding 5 PVU on 9 February 2023, at 1200Z (figure not shown). This was associated with a surface low-pressure system, an upper air trough and a strong jet stream. During this period, the PV contours elongated predominantly from south to north over the western regions of the surface low-pressure system as the jet stream shifted into the baroclinic westerly wave trough. High absolute PV values are typical in COL systems, where low pressure progressively develops and extends towards the surface.

Significantly, the formation of the 500-hPa COL on 10 February 2023 marked the initiation of dynamic processes extending to lower levels, which are crucial for subsequent cyclogenesis phases (Hoskins et al., 1985). Furthermore, analysis from the MERRA-2 database for upper level ozone mixing ratios at this altitude indicated elevated ozone mixing ratios (15×10^{-9} kg/kg) over the study area during this period (figures are not shown). Danielsen (1968) demonstrated a significant correlation between ozone mixing ratios and potential vorticity. Figure 7a depicts the average upper level potential vorticity at 300 hPa from 6 February 2023 at 0000Z to 14 February 2023 at 2300Z across the study area. This figure illustrates negative (southern hemisphere) potential vorticity at 300 hPa, indicative of developing and potentially intensifying low-pressure systems. The highest average PV value at 300 hPa during this period was -1.44×10^{-6} km^2 kg^{-1} s^{-1}, primarily observed in the western regions of South Africa.

Simultaneously, the highest ozone mixing ratio recorded during this period was 12.6×10^{-8} kg/kg over the mentioned region (Figure 7b).

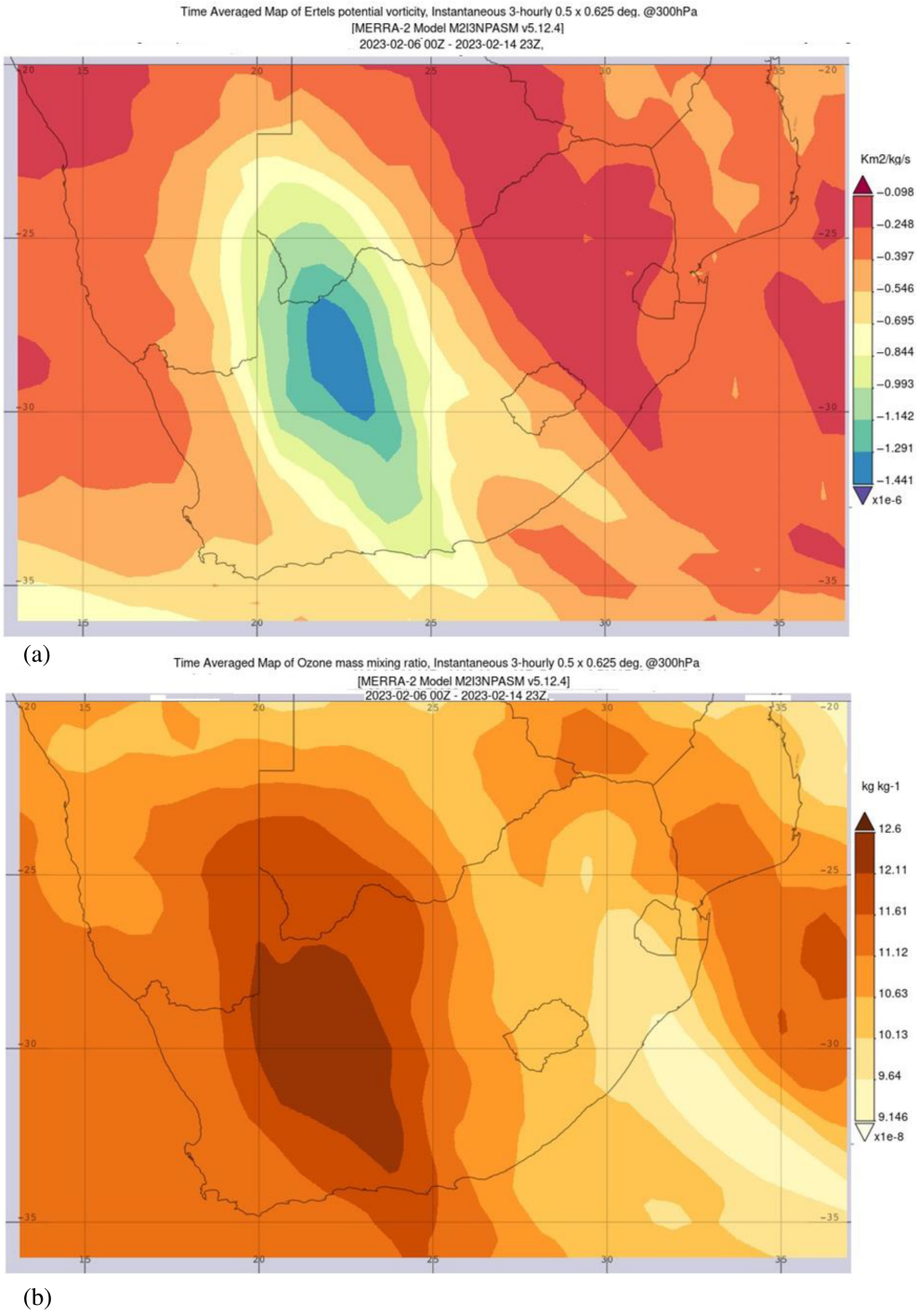

FIGURE 7 Ertel potential vorticity (a) and ozone mixing ratio at 300 hPa (b) for the period from 6 to 14 February 2023.

4.4 | Abnormal weather patterns associated with the COL

Figure 8a shows the geopotential height at a level of 700 hPa. The isotherms at level 700 hPa are depicted in Figure 8b from 10 to 11 February 2023, during the active COL over the study. Figure 8c,d show the geopotential heights at 850 hPa and air temperatures at 850 hPa respectively. Figure 8e,f display the geopotential height at 925 hPa and its isotherms correspondingly during the active COL over the study area. These figures together denote the development of the COL associated with the cold core extending from the south-high latitudes toward the central and eastern parts of South Africa. This has reached the surface, which is associated with surface dynamical depression (see Figure 5). A COL typically begins as an upper air trough (westerly wave), closing off and descending to the surface as a low-pressure system with a cold pool. Circular isotherms around the low core illustrate a COL's presence (see Figure 8). These figures

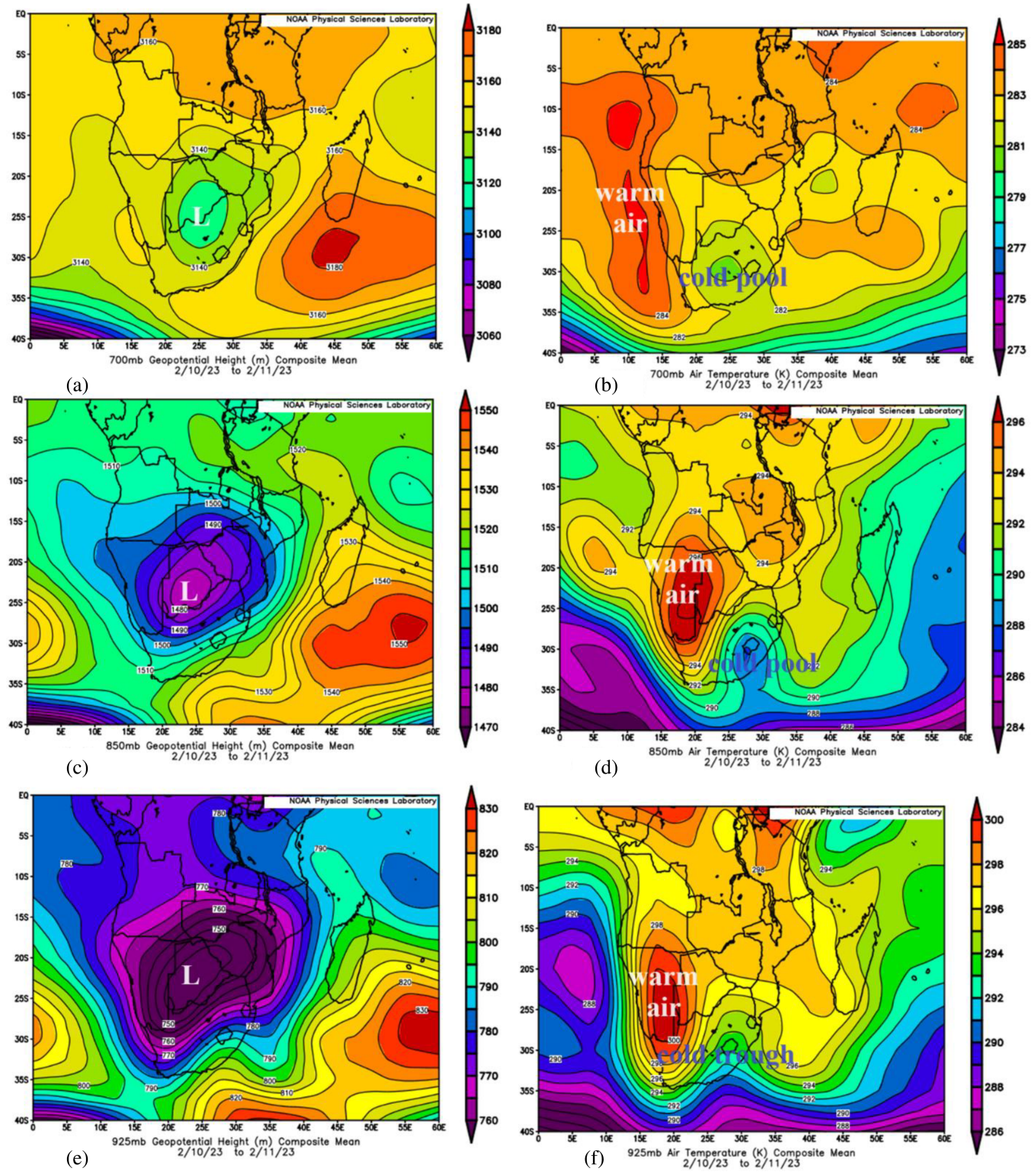

FIGURE 8 Geopotential height at 700 hPa (a), isotherms at 700 hPa (b), geopotential heights at 850 hPa (c), isotherms at 850 hPa (d), 925 hPa geopotential heights (e) and the isotherms at 925 hPa (f) during the active cutoff low (COL) over the study area.

highlight that the COL forms under blocking high-pressure conditions, resulting in a slow-moving system persisting across the study area and leading to widespread heavy rainfall, primarily over the eastern and northeastern provinces of South Africa. Moreover, as these figures show, the dynamic low originating from the south has interacted with the seasonal Angola heat low in a barotropic manner. This interaction is associated

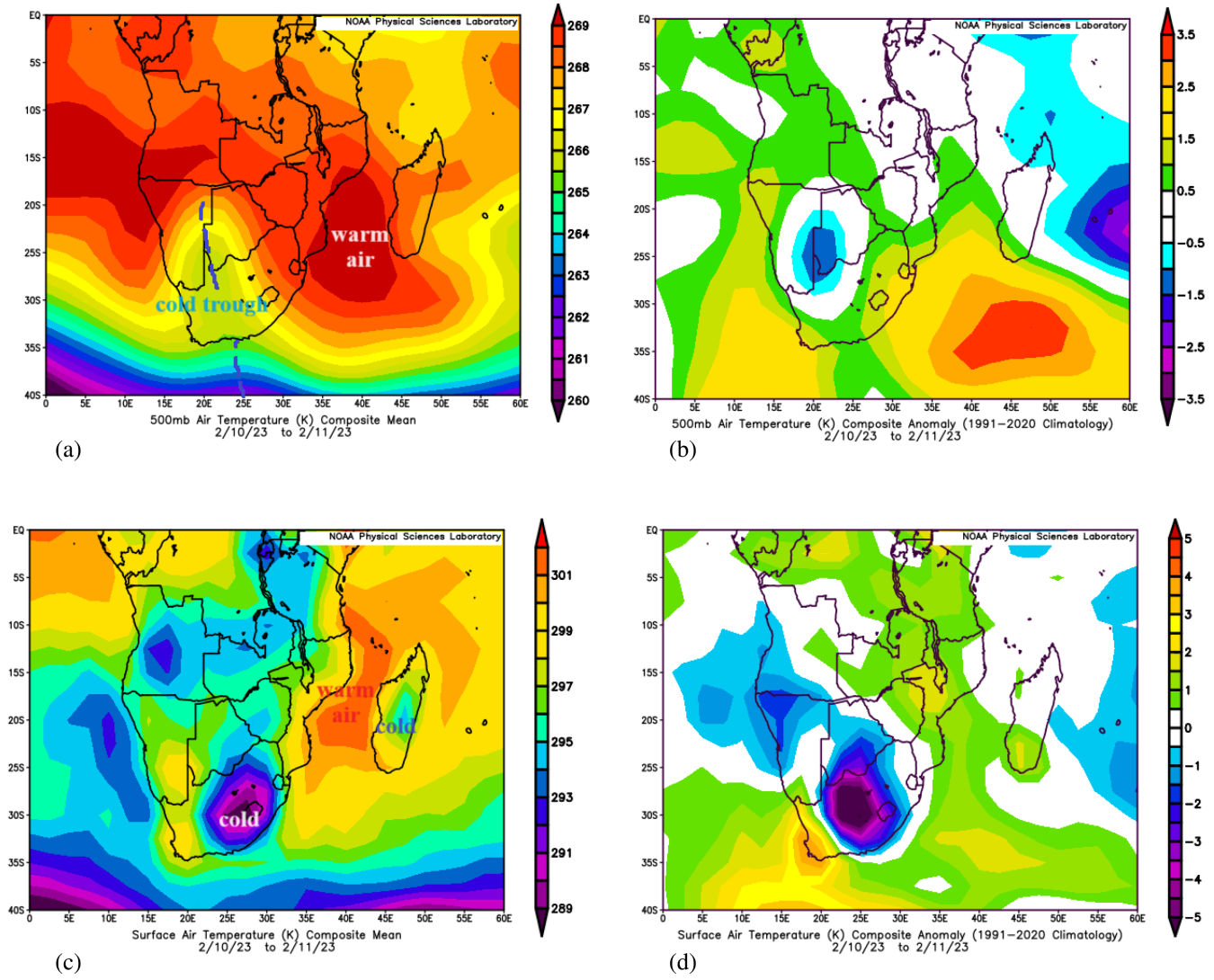

FIGURE 9 Air temperatures at 500 hPa (a), anomalies of the air temperatures at 500 hPa (b), surface air temperatures (c) and surface air temperature anomalies (d) during the active cutoff low (COL) over the study area.

with a warm air column extending to 700 hPa (Figure 8b,d,f). COL typically initiates as an upper air trough (westerly wave), closing off and descending to the surface as a low-pressure system with a cold pool.

Figure 9a shows the 500-hPa air temperatures during the active COL over the study area. This figure denotes a cold trough extending from the south-high latitudes toward the western and central parts of South Africa, eastern Namibia and western Botswana. Figure 9b indicates that the isotherm anomalies exhibit a normal departure from climate norms at 500 hPa. The figure illustrates colder air temperatures with a maximum anomaly of 1.5 K in the west and warmer air temperatures with a maximum anomaly of 3.5 K at the 500 hPa level over the Indian Ocean below Madagascar. In Figure 9c, the surface air temperature map during the active operation of the COL has been shown. This figure shows cold core air temperatures mostly over central and eastern South Africa, situated between warmer air in western South Africa and the upper eastern boundaries extending to the Mozambique Channel. Figure 9d represents the anomaly map for Figure 9c, indicating significantly colder surface air temperatures of less than approximately 5 K over most parts of South Africa, except for small areas in the southwest with warmer surface air and some parts in the northeast showing no change.

Figure 10 shows the low-level relative humidity at 850 hPa (a), its anomaly map departure from the climate normal (b) and the vertical pressure velocity (omega) at 500 hPa (c). The anomaly map for the omega at 500 hPa has been brought in Figure 10d. Figure 10a shows that the humidity changes from ~70% to 90% over the central and eastern areas of South Africa, which has abnormally increased by ~10%–20% (Figure 10b). This, along with

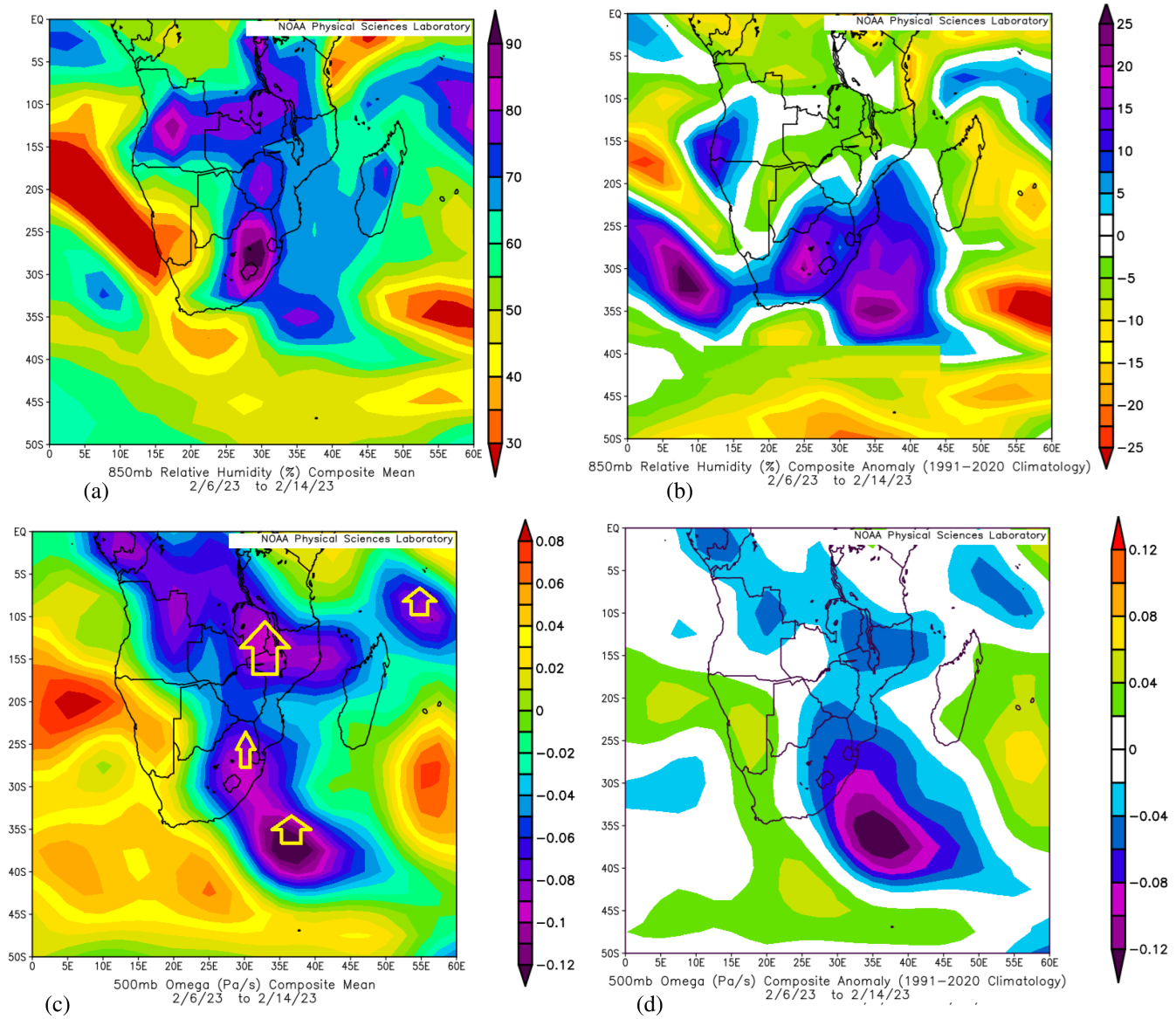

FIGURE 10 Low-level relative humidity at 850 hPa (a), the anomaly map for panel a departure from climate normal (b), the vertical pressure velocity (omega) at 500 hPa (c) and anomalies of panel c (d).

the strong vertical motion (yellow arrow) in the study area (Figure 10c), intensified in comparison to the normal climate values during the extreme event in the study area. Considering the low-level humid air (Figure 10a), the more intense moisture from the Mozambique Channel moved and then lifted upward (negative omega), resulting in strong convection over the study area during extreme precipitation. Therefore, convections are mostly produced to the north and east of the surface low-pressure system (see Figure 5). Convective clouds can occur east of easterly waves. With the southward shift of the SICZ from austral summer to southern African northern areas, easterly waves can form along with the continental heat low-pressure system in these areas. Therefore, due to the cold low at low levels (Figure 8b,d, f) in the eastern areas of South Africa and the warmer air at 500 hPa (Figure 9a), convection was sustained by the latent heat released by condensation. Because of the low-level cold core and upper warm core, the cyclonic vorticity increases from the surface to 850 hPa and then decreases with height. Figure 11 shows the anomaly pattern for low-level (850 hPa) meridional (a) and zonal (b) winds over the study area during the study period. This figure shows abnormal easterly winds along with northern flows from warmer (Figure 9d) water carrying abnormally more low-level moisture (Figure 10b) to the study area. The wind component along the local (zonal) meridian is recognized from the zonal (meridional) wind. This figure shows that the easterly wave predominates over warm sea surface temperature areas with notable

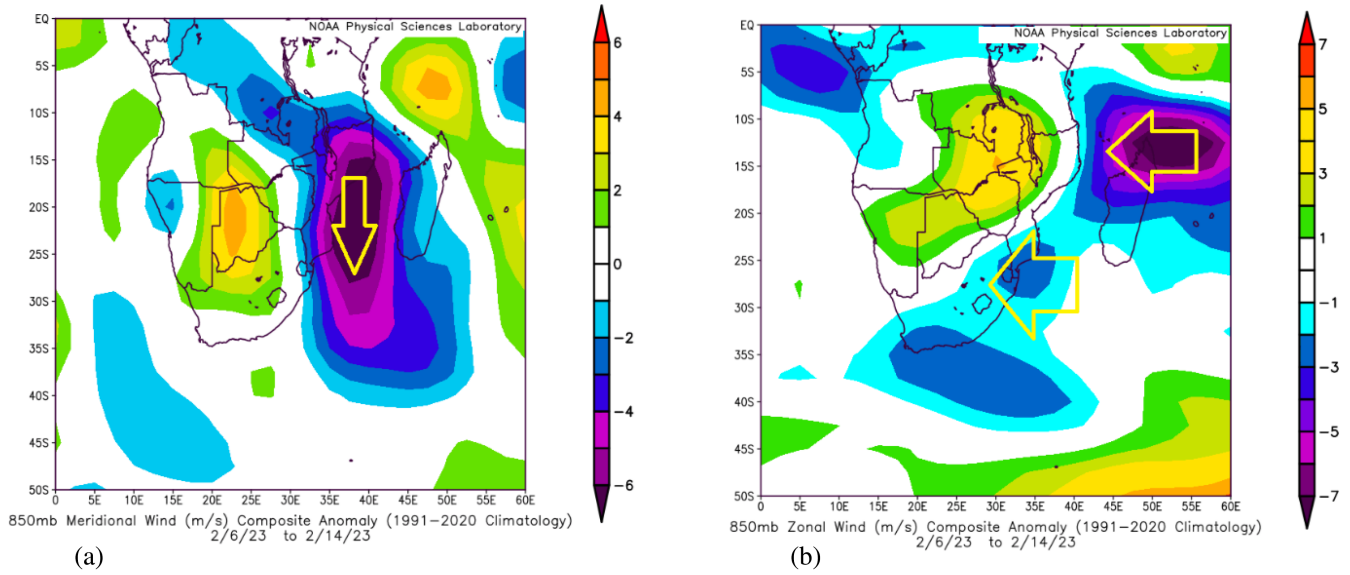

FIGURE 11 Low-level (850 hPa) anomalies of the meridional (a) and zonal (b) winds over the study area during the study period.

abnormal meridional humidity gradients (Figures 10b and 11a). It is noted that the anomalous meridional winds impact the SICZ mean meridional moisture gradient, which causes moisture anomalies to enhance convection on the trough side of the easterly wave (Rydbeck & Maloney, 2015). However, the rainfall within the SICZ is supported by not only meridional wind but also zonal wind convergence (Cook, 2000) as noticed in Figure 11b.

4.5 | Easterly and westerly waves coupling during extreme events

Figure 12 depicts the average wind vector field at 850 hPa during 6–14 February 2023 over the study area (a) and its anomaly map (b), showing departures from the climate normal (1991–2020). Yellow lines in Figure 12a indicate inverted troughs at 850 hPa, with black lines highlighting wind curvatures in specific areas for clarity. It illustrates an elongated inverted trough over northeastern Madagascar (yellow line), connected to the SICZ, and another inverted trough mainly developing east of Angola. These troughs are associated with cyclonic circulations that form seasonally on both sides of the anticyclonic ridge influenced by easterly currents. The cyclonic curvature is linked to the presence of a low-pressure cyclonic system, such as the Angola heat low (Figure 5), which fosters easterly wave formation. Figure 12a shows that during this period, the propagation of easterly waves (in the easterly trades) impacted the region, followed by an induced trough accompanying the westerly system aloft (referenced in Figure 4 for 500 hPa geopotential height), intensifying the occurrence of heavy precipitation and flooding across the study area. This phenomenon can be attributed to the inflow of warmer, more humid air from the northern tropics, as detailed in the subsequent figures.

Similar atmospheric patterns (Figure 12) are observed at 700 hPa (figure not shown). The perturbations propagate westward along the easterly trade winds, indicating a trough with increased cyclonic vorticity at 850 and 700 hPa. Due to the barotropic nature of this system, enhanced convection and heavy precipitation are associated with it (see following figures). Notably, easterly waves gradually dissipate over the Atlantic Ocean, often reinitiating east of Mozambique.

Figure 12b highlights abnormal structures observed in Figure 12a. This figure illustrates significantly intensified easterlies and northerly winds, reaching a maximum of 9 m/s through the Mozambique Channel towards eastern South Africa, alongside heightened cyclonic winds (~8 m/s) over eastern Angola (indicated by red arrow). These abnormal wind patterns during the coupling of westerly and easterly waves deviate from normal conditions during 6–14 February 2023, contributing to heavy precipitation and subsequent flooding in the study area. Figure 12c briefly shows a schematic diagram to display the mechanisms associated with the extreme precipitation event. In this diagram, MCT, COL and SICS represent the Mozambique Channel, cutoff low and South Indian Ocean Convergence Zone respectively.

5 | SUMMARY AND CONCLUDING REMARKS

This study investigates the meteorological mechanisms behind the heavy rainfall experienced in southeastern

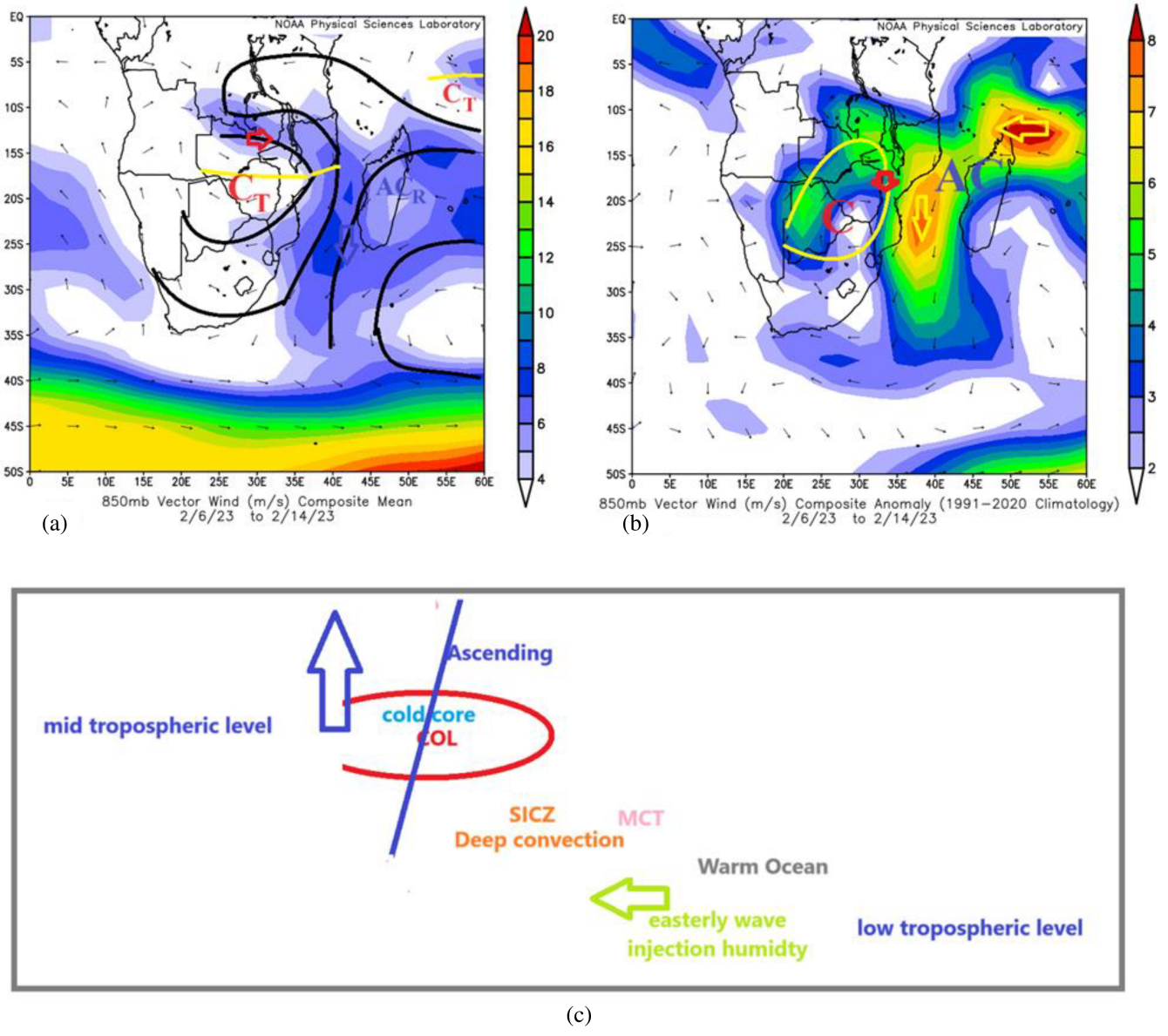

FIGURE 12 An averaged wind vector field at a level of 850 hPa (a), the anomaly map for panel a (b) and a schematic diagram to display the mechanisms associated with the extreme precipitation event during 6–14 February 2023 over the study area.

Africa from 6 to 14 February 2023. The focus was on southern Mozambique and southern Africa's eastern and northeastern areas, including Limpopo, Mpumalanga and northern KwaZulu-Natal. This weather system caused severe disturbances, persistence and heavy rainfall throughout the region. The results have revealed the rainfall within the SICZ is supported by not only meridional wind (within SICZ) but also zonal wind convergence. Therefore, the SICZ deep convection area associated with disturbances drove moisture into the easterly wave, coupled with a converted westerly wave to a COL system. This study revealed an abnormal structural pattern in the wind vectors, low-pressure trough, upper and mid-tropospheric westerly flows and humidity compared with the long-term climate average values over Mozambique and the northeastern and eastern regions of southern Africa. By analysing various datasets, including outputs from reanalysis, it was determined that a slow-moving upper air COL system over central South Africa was critical in triggering extensive and heavy rainfall in these regions. The interaction between a near-stationary upper air COL system and an easterly wind wave from SICZ injected significant warm, humid air from the Indian Ocean, resulting in severe disturbances and persistent heavy rainfall. The study's findings are of two significant importance factors. Firstly, the persistent COL system over central South Africa was identified as the primary driver of the heavy rainfall, a crucial insight for weather

forecasting. Secondly, the coupling between an initiated westerly wave, which converted to the upper-air COL system, and the easterly wind wave associated with the SICZ was crucial in bringing warm, humid air into the region. This understanding can aid in disaster preparedness.

Additionally, the study observed abnormal structural patterns in wind vectors, low-pressure troughs, upper and mid-tropospheric westerly flows and humidity compared with long-term climate averages, providing a unique perspective on climate change impacts. Furthermore, the intensity and duration of the event, coupled with cyclonic activity, underscore the impacts of climate change on weather patterns in southern Africa. The heavy rainfall led to significant flooding and disruptions, emphasizing the need for improved forecasting models and disaster preparedness strategies.

The study, however, has certain areas for improvement. It relied on reanalysis data, which, while comprehensive, may have inherent biases and limitations in spatial and temporal resolution. More ground-based observational data also needed to be collected to validate the model outputs fully. Additionally, the focus was on specific regions within southern Mozambique and northeastern South Africa, and other potentially affected areas were not thoroughly examined.

Addressing the study's limitations by enhancing data collection efforts, particularly by increasing the density of ground-based observational networks to provide more accurate and localized data, can lead to more precise forecasting. Additional research is required to comprehend the long-term effects of climate change on the occurrence and severity of similar weather events, thereby paving the way for improved disaster preparedness. Improving and refining models to better capture the interactions between different weather systems, especially in the context of climate variability and change, will also be crucial. Moreover, expanding the study to include other regions affected by similar weather patterns assists in developing a comprehensive understanding of these phenomena, inspiring a more holistic approach to weather research.

AUTHOR CONTRIBUTIONS

Farahnaz Fazel-Rastgar: Conceptualization; data curation; formal analysis; visualization; writing – original draft; methodology; investigation; supervision; project administration; writing – review and editing; software; validation; funding acquisition; resources. **Venkataraman Sivakumar:** Conceptualization; data curation; methodology; investigation; supervision; project administration; writing – review and editing; validation; funding acquisition; resources; software; writing – original draft. **Masoud Rostami:** Conceptualization; data curation; formal analysis; writing – original draft; methodology; investigation; supervision; project administration; writing – review and editing; software; validation; funding acquisition; resources. **Bijan Fallah:** Conceptualization; data curation; validation; methodology; investigation; formal analysis; writing – review and editing.

ACKNOWLEDGEMENTS

Thanks are given to the NOAA/ESRL PSD, Physical Science Division, Boulder Colorado web page through http://www.esrl.noaa.gov/psd/ and Giovanni online data system, developed and maintained by the NASA GES DISC and NASA LP DAAC at the USGS EROS Center and EUMETSAT for providing the archive images. Thanks to the South African Weather Service for providing the precipitation data. The authors would like to thank the anonymous reviewers for their valuable comments and suggestions. The authors gratefully acknowledge the support from Virgin Unite USA, Inc. through the Planetary Boundary Science Lab project, the European Regional Development Fund (ERDF), the German Federal Ministry of Education and Research and the Land Brandenburg.

FUNDING INFORMATION

This research was funded by the Virgin Unite USA, Inc. through the Planetary Boundary Science Lab project.

CONFLICT OF INTEREST STATEMENT

The authors declare no conflicts of interest.

DATA AVAILABILITY STATEMENT

Data sharing is not applicable to this article as no new data were created or analyzed in this study.

ORCID

Farahnaz Fazel-Rastgar https://orcid.org/0000-0002-3904-4313

Masoud Rostami https://orcid.org/0000-0003-1730-5145

REFERENCES

Barimalala, R., Blamey, R.C., Desbiolles, F. & Reason, C.J. (2020) Variability in the Mozambique Channel trough and impacts on southeast African rainfall. *Journal of Climate*, 33(2), 749–765.

Barimalala, R., Desbiolles, F., Blamey, R.C. & Reason, C. (2018) Madagascar influence on the South Indian Ocean convergence zone, the Mozambique Channel trough and southern African rainfall. *Geophysical Research Letters*, 45(20), 11–380.

Barnes, M.A., Turner, K., Ndarana, T. & Landman, W.A. (2021) Cape storm: a dynamical study of a COL and its impact on South Africa. *Atmospheric Research*, 249, 105290.

Britannica, T. & Editors of Encyclopaedia. (2023) *Mozambique current. Encyclopedia Britannica*. Available from: https://www.britannica.com/place/Mozambique-Current

Burpee, R.W. (1972) The origin and structure of easterly waves in the lower troposphere of North Africa. *Journal of the Atmospheric Sciences*, 29(1), 77–90. Available from: https://doi.org/10.1175/1520-0469(1972)029<0077:toasoe>2.0.co;2

Carvalho, L.M., Jones, C. & Liebmann, B. (2004) The south Atlantic convergence zone: intensity, form, persistence, and relationships with Intraseasonal to interannual activity and extreme rainfall. *Journal of Climate*, 17(1), 88–108. Available from: https://doi.org/10.1175/1520-0442(2004)017<0088:tsaczi>2.0.co;2

Chang, J.-H. (1972) *Atmospheric circulation systems and climate*. Honolulu: Oriental Publishing Co.

Cook, K.H. (2000) The south Indian convergence zone and interannual rainfall variability over southern Africa. *Journal of Climate*, 13(21), 3789–3804.

Danielsen, E.F. (1968) Stratospheric-tropospheric exchange based on radioactivity, ozone and potential vorticity. *Journal of Atmospheric Sciences*, 25(3), 502–518.

Dieppois, B., Pohl, B., Rouault, M., New, M., Lawler, D. & Keenlyside, N. (2016) Interannual to interdecadal variability of winter and summer southern African rainfall, and their teleconnections. *Journal of Geophysical Research: Atmospheres*, 121(11), 6215–6239.

Fallah, B., Didovets, I., Rostami, M. & Hamidi, M. (2024) Climate change impacts on Central Asia: trends, extremes and future projections. *International Journal of Climatology*, 44, 3191–3213.

Fallah, B. & Rostami, M. (2024) Exploring the impact of the recent global warming on extreme weather events in Central Asia using the counterfactual climate data ATTRICI v1.1. *Climatic Change*, 177(5), 80.

Fallah, B., Russo, E., Menz, C., Hoffmann, P., Didovets, I. & Hattermann, F.F. (2023) Anthropogenic influence on extreme temperature and precipitation in Central Asia. *Scientific Reports*, 13, 6854.

Fazel-Rastgar, F. & Sivakumar, V. (2022) A severe weather system accompanied by a stratospheric intrusion during unusual warm winter in 2015 over the South Africa: an initial synoptic analysis. *Remote Sensing Applications: Society and Environment*, 28, 100833. Available from: https://doi.org/10.1016/j.rsase.2022.100833

Hersbach, H., Bell, B., Berrisford, P., Dahlgren, P., Horányi, A., Muñoz-Sabater, J. et al. (2020) The ERA5 global reanalysis: achieving a detailed record of the climate and weather for the past 70 years. *The ERA5 Global Reanalysis*, 146, 1999–2049. Available from: https://doi.org/10.5194/egusphere-egu2020-10375

Hoell, A., Funk, C., Zinke, J. & Harrison, L. (2017) Modulation of the southern Africa precipitation response to the El Niño Southern Oscillation by the subtropical Indian Ocean dipole. *Climate Dynamics*, 48, 2529–2540.

Hoskins, B.J., McIntyre, M.E. & Robertson, A.W. (1985) On the use and significance of isentropic potential vorticity maps. *Quarterly Journal of the Royal Meteorological Society*, 111(470), 877–946. Available from: https://doi.org/10.1002/qj.49711147002

Hulme, M. (1992) Rainfall changes in Africa: 1931–1960 to 1961–1990. *International Journal of Climatology*, 12(7), 685–699. Available from: https://doi.org/10.1002/joc.3370120703

Kalnay, E., Kanamitsu, M., Kistler, R., Collins, W., Deaven, D., Gandin, L. et al. (1996) The NCEP/NCAR 40-year reanalysis project. *Bulletin of the American Meteorological Society*, 77(3), 437–471. Available from: https://doi.org/10.1175/1520-0477(1996)077<0437:tnyrp>2.0.co;2

Kiladis, G.N., Von Storch, H. & Loon, H. (1989) Origin of the South Pacific convergence zone. *Journal of Climate*, 2(10), 1185–1195. Available from: https://doi.org/10.1175/1520-0442(1989)002<1185:ootspc>2.0.co;2

Landman, W.A. & Mason, S.J. (1999) Change in the association between Indian Ocean sea-surface temperatures and summer rainfall over South Africa and Namibia. *International Journal of Climatology: A Journal of the Royal Meteorological Society*, 19(13), 1477–1492.

Nicholson, S. (2003) Comments on "The South Indian convergence zone and interannual rainfall variability over southern Africa" and the question of ENSO's influence on southern Africa. *Journal of Climate*, 16(3), 555–562.

Ordóñez, P., Ribera, P., Gallego, D. & Peña-Ortiz, C. (2012) Major moisture sources for Western and Southern India and their role on synoptic-scale rainfall events. *Hydrological Processes*, 26(25), 3886–3895.

Rapolaki, R., Blamey, R., Hermes, J. & Reason, C. (2021) Moisture sources and transport during an extreme rainfall event over the Limpopo river basin, Southern Africa. *Atmospheric Research*, 264, 105849. Available from: https://doi.org/10.1016/j.atmosres.2021.105849

Reason, C.J.C. (2017) *Climate of southern Africa. Oxford research encyclopedia of climate science*. Available from: https://oxfordre.com/climatescience/view/10.1093/acrefore/9780190228620.001.0001/acrefore-9780190228620-e-513

Reason, C.J.C. & Mulenga, H. (1999) Relationships between south African rainfall and SST anomalies in the southwest Indian Ocean. *International Journal of Climatology: A Journal of the Royal Meteorological Society*, 19(15), 1651–1673.

Riehl, H. (1944) *Waves in the easterlies and the polar front in the tropics: a report on research conducted at the institute of tropical meteorology of the university of Chicago at the university of Puerto Rico, Rio Piedras, PR (No. 17)*. Chicago, IL: University of Chicago Press.

Rienecker, M.M., Suarez, M.J., Gelaro, R., Todling, R., Bacmeister, J., Liu, E. et al. (2011) MERRA: NASA's modern-era retrospective analysis for research and applications. *Journal of Climate*, 24(14), 3624–3648. Available from: https://doi.org/10.1175/jcli-d-11-00015.1

Rostami, M. & Zeitlin, V. (2021) Instabilities of low-latitude easterly jets in the presence of moist convection and topography and related cyclogenesis, in a simple atmospheric model. *Geophysical & Astrophysical Fluid Dynamics*, 116(1), 56–77.

Rydbeck, A.V. & Maloney, E.D. (2015) On the convective coupling and moisture organization of east Pacific easterly waves. *Journal of the Atmospheric Sciences*, 72(10), 3850–3870.

Seo, H., Jochum, M., Murtugudde, R., Miller, A.J. & Roads, J.O. (2008) Precipitation from African easterly waves in a coupled model of the tropical Atlantic. *Journal of Climate*, 21(6), 1417–1431.

Singleton, A.T. & Reason, C.J.C. (2007a) A numerical model study of an intense COL pressure system over South Africa. *Monthly*

Weather Review, 135(3), 1128–1150. Available from: https://doi.org/10.1175/mwr3311.1

Singleton, A.T. & Reason, C.J.C. (2007b) Variability in the characteristics of cut-off low pressure systems over subtropical southern Africa. *International Journal of Climatology: A Journal of the Royal Meteorological Society*, 27(3), 295–310.

Sivakumar, V. & Fazel-Rastgar, F. (2021) Heavy rainfall resulting from extreme weather disturbances in eastern coastal parts of South Africa: 11 April 2022. In *Proceedings of the earth and environmental sciences international webinar conference*. Cham: Springer International Publishing, pp. 161–186.

Tai, K.S. & Ogura, Y. (1987) An observational study of easterly waves over the eastern Pacific in the northern summer using FGGE data. *Journal of the Atmospheric Sciences*, 44(2), 339–361.

Todd, M. & Washington, R. (1999) Circulation anomalies associated with tropical-temperate troughs in southern Africa and the south west Indian Ocean. *Climate Dynamics*, 15(12), 937–951.

Weldon, D. & Reason, C.J.C. (2014) Variability of rainfall characteristics over the south coast region of South Africa. *Theoretical and Applied Climatology*, 115, 177–185.

Xulu, N.G. (2017) *Impact of spatiotemporal variability of the Mascarene High on weather and climate over southern Africa* (Doctoral dissertation).

Xulu, N.G., Chikoore, H., Bopape, M.J.M. & Nethengwe, N.S. (2020) Climatology of the mascarene high and its influence on weather and climate over southern Africa. *Climate*, 8(7), 86.

Xulu, N.G., Chikoore, H., Bopape, M.M., Ndarana, T., Muofhe, T.P., Mbokodo, I.L. et al. (2023) COL s over South Africa: a review. *Climate*, 11(3), 59. Available from: https://doi.org/10.3390/cli11030059

How to cite this article: Fazel-Rastgar, F., Sivakumar, V., Rostami, M., & Fallah, B. (2025). Unveiling meteorological synergies in the coupling of an abnormal easterly wave and cutoff low in South Africa's February 2023 rainfall. *Meteorological Applications*, *32*(1), e70027. https://doi.org/10.1002/met.70027